

**Two-photon-exchange effects in the unpolarized  $\mu p$  scattering within a hadronic model**

Hai-Qing Zhou\*

*Department of Physics, Southeast University, NanJing 211189, China*  
*and State Key Laboratory of Theoretical Physics, Institute of Theoretical Physics, Chinese Academy of Sciences,*  
*Beijing 100190, People's Republic of China*

(Received 16 October 2016; published 13 February 2017)

In this work, the two-photon-exchange (TPE) effects in the unpolarized  $\mu p$  scattering are discussed within the hadronic model where the intermediate states  $N$ ,  $\Delta$ , and  $\sigma$  are considered. The contribution from the  $N$  intermediate is close to the results given by Tomalak and Vanderhaeghen [Phys. Rev. D **90**, 013006 (2014)] at small  $Q$ , and there is a sizable difference when  $Q > 0.25$  GeV (where  $Q^2$  is the four-momentum transfer). The contributions from the  $\Delta$  and the  $\sigma$  intermediate states are much smaller than that from the  $N$  intermediate at small  $Q$ . In the kinematic region with  $k_i \subseteq [0.01, 0.3]$  GeV and  $Q \leq 0.4$  GeV (where  $k_i$  is the three-momentum of initial muon in the laboratory frame), a naive expression for the TPE contributions is given, which can be used directly for other analysis.

DOI: 10.1103/PhysRevC.95.025203

**I. INTRODUCTION**

The two-photon-exchange (TPE) effects in elastic  $ep$  scattering have been widely studied (see the recent review papers [1,2]) after 2000 to explain the discrepancy between the measurements of  $R = \mu G_E/G_M$  (with  $G_{E,M}$  the electromagnetic form factors of the proton) by the Reosenbluth method [3,4] and the polarized method [5,6]. After the appearance of the proton radius puzzle [7,8], the TPE effects in the  $\mu p$  system also gave rise to several interesting papers [9–12]. The coming experiment MUSE [13] proposes the measurement of the electromagnetic form factors of the proton by elastic unpolarized  $\mu p$  scattering at small momentum transfer and the aim of the precise extraction of the form factors calls for the careful consideration of the TPE effects.

In the literature, many methods have been applied to estimate the TPE effects in  $ep$  and  $\mu p$  scattering, for example, for example, the hadronic model [14–18], the generalized parton distributions (GPD's) method [19,20], the phenomenological parametrizations [21,22], the dispersion relation approach [23–27], the perturbative QCD (pQCD) calculations [28,29], and the soft-collinear effective theory (SCEF) method [30]. Among these methods, the hadronic model is usually used in small and medium momentum transfers. With this method, the TPE contribution in  $\mu p$  scattering from the intermediate  $N$  was estimated in Refs. [17,18], and recently the contribution from the  $\sigma$  meson exchange in the  $t$  channel was also discussed in Ref. [31]. In this work, I give an estimation of the TPE effects in a  $\mu p$  system from the intermediate state  $\Delta$ , and the contributions from the  $N$  and the  $\sigma$  intermediate states are also discussed. Furthermore, I give a naive formula to express these contributions, which can be used directly for other analysis. In Sec. II I give a brief introduction of the model, in Sec. III I list the input parameters I used, in Sec. IV I present the numerical results, and finally I give a discussion and a short summary.

**II. BASIC FORMULA**

In the Feynman gauge, the amplitude for  $\mu p$  scattering in the Born approximation shown in Fig. 1 can be expressed as

$$i\mathcal{M}_{\mu p}^{1\gamma} = \bar{u}(p_3, m_\mu)(-ie\gamma_\mu)u(p_1, m_\mu)\bar{u}(p_4, m_N) \times \Gamma_{\gamma NN}^\mu u(p_2, m_N)S_\gamma(q), \quad (1)$$

where  $p_1, p_3$  are the momenta of the incoming and outgoing muons,  $p_2, p_4$  are the momenta of the incoming and outgoing protons,  $m_\mu, m_N$  are the masses of muon and proton,  $e = -|e|$ ,  $\Gamma_{\gamma NN}^\mu$  is the effective vertex for the  $\gamma NN$  interaction,  $q \equiv p_1 - p_3$ , and

$$S_\gamma(q) = \frac{-i}{q^2 + i\epsilon}.$$

The TPE amplitude in  $\mu p$  scattering can generally be expressed as

$$i\mathcal{M}_{\mu p}^{2\gamma} = \int \frac{d^4\bar{k}}{(2\pi)^4} L_{\mu p}^{\mu\nu} H_{\mu p, \mu\nu}, \quad (2)$$

where  $L_{\mu p}^{\mu\nu}$  is the amplitude for the double virtual Compton scattering of the muon which can be written explicitly, and  $H_{\mu p, \mu\nu}$  is the amplitude for the double virtual Compton scattering of the proton. Owing to the nonperturbative properties of QCD, the explicit expression for  $H_{\mu p, \mu\nu}$  in the entire kinematical region is unknown. In the very low-momentum region, this amplitude can be estimated by chiral perturbation theory, and in the deep virtual region, it can be estimated by the GPD, pQCD, or SCEF methods. In the medium momentum transfer region, an estimation based on the hadronic level has to be applied.

At the hadronic level, I separate the contributions to the double virtual Compton scattering into four kinds as the  $s$  channel,  $u$  channel,  $t$  channel, and the other contributions.

\*zhouhq@seu.edu.cn

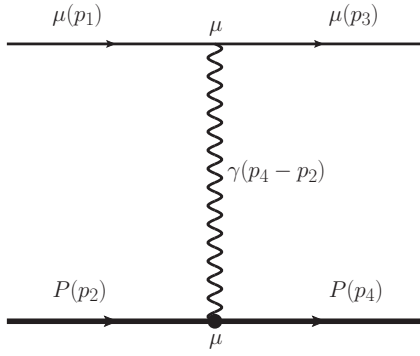


FIG. 1. One-photon-exchange diagram for  $\mu p$  scattering in the Feynman gauge.

In this work, I limit the discussion to the former three kinds of contributions, and in the  $s$  and  $u$  channels, I only considered the  $N$  and the  $\Delta$  intermediate states; in the  $t$  channel, I only consider the  $\sigma$  meson exchange.

#### A. TPE contributions from $N, \Delta$ intermediate states in the $s$ and $u$ channels

At the hadronic level, the diagrams for the TPE amplitudes in the  $s$  and  $u$  channels of  $\mu p$  scattering are shown in Fig. 2, where the intermediate states are proton and  $\Delta$ .

In my estimation, I take the corresponding effective vertexes as

$$\begin{aligned} \Gamma_{\gamma NN}^{\mu}(\bar{q}) &= ie \left\{ F_1(\bar{q}^2) \gamma^{\mu} + i \sigma^{\mu\nu} \frac{F_2(\bar{q}^2)}{2m_N} q_{\nu} \right\}, \\ \Gamma_{\gamma \Delta \rightarrow N}^{\mu\alpha}(\bar{p}, \bar{q}) &= -i \sqrt{\frac{2}{3}} \frac{e}{2m_{\Delta}^2} \left\{ g_1 F_{\Delta}^{(1)}(\bar{q}^2) [g^{\mu\alpha} \bar{p} \bar{q} - \bar{p}^{\mu} \gamma^{\alpha} \bar{q} - \gamma^{\mu} \gamma^{\alpha} \bar{p} \cdot \bar{q} + \gamma^{\mu} \bar{p} \bar{q}^{\alpha}] + g_2 F_{\Delta}^{(2)}(\bar{q}^2) [\bar{p}^{\mu} \bar{q}^{\alpha} - g^{\mu\alpha} \bar{p} \cdot \bar{q}] \right. \\ &\quad \left. + (g_3/M_{\Delta}) F_{\Delta}^{(3)}(\bar{q}^2) [\bar{q}^2 (\bar{p}^{\mu} \gamma^{\alpha} - g^{\mu\alpha} \bar{p}) + \bar{q}^{\mu} (\bar{q}^{\alpha} \bar{p} - \gamma^{\alpha} \bar{p} \cdot \bar{q})] \right\} \gamma_5, \\ \Gamma_{\gamma N \rightarrow \Delta}^{\nu\beta}(\bar{p}, \bar{q}) &= -i \sqrt{\frac{2}{3}} \frac{e}{2m_{\Delta}^2} \gamma_5 \left\{ g_1 F_{\Delta}^{(1)}(\bar{q}^2) [g^{\nu\beta} \bar{q} \bar{p} - p^{\nu} \bar{q} \gamma^{\beta} - \gamma^{\beta} \gamma^{\nu} \bar{p} \cdot \bar{q} + \bar{p} \gamma^{\nu} \bar{q}^{\beta}] + g_2 F_{\Delta}^{(2)}(\bar{q}^2) [\bar{p}^{\nu} \bar{q}^{\beta} - g^{\nu\beta} \bar{p} \cdot \bar{q}] \right. \\ &\quad \left. - (g_3/m_{\Delta}) F_{\Delta}^{(3)}(\bar{q}^2) [\bar{q}^2 (\bar{p}^{\nu} \gamma^{\beta} - g^{\nu\beta} \bar{p}) + \bar{q}^{\nu} (\bar{q}^{\beta} \bar{p} - \gamma^{\beta} \bar{p} \cdot \bar{q})] \right\}, \end{aligned} \quad (3)$$

with  $\bar{q}, \bar{p}$  the momenta of the incoming photon and proton or  $\Delta$ ,  $m_{\Delta}$  the mass of the  $\Delta$ , and  $F_{1,2}, F_{\Delta}^{(1,2,3)}$  the corresponding form factors.

With these effective vertexes, the corresponding amplitudes in the Feynman gauge can be written explicitly as

$$\begin{aligned} i\mathcal{M}_{\mu p}^{(a)} &= \int \frac{d^4 k}{(2\pi)^4} \bar{u}(p_3, m_{\mu}) (-ie\gamma_{\mu}) S_{\mu}(p_1 + p_2 - k) (-ie\gamma_{\nu}) u(p_1, m_{\mu}) S_{\gamma}(p_4 - k) S_{\gamma}(k - p_2) \\ &\quad \times \bar{u}(p_4, m_N) \Gamma_{\gamma NN}^{\mu}(p_4 - k) S_p(k) \Gamma_{\gamma NN}^{\nu}(k - p_2) u(p_2, m_N), \\ i\mathcal{M}_{\mu p}^{(b)} &= \int \frac{d^4 k}{(2\pi)^4} \bar{u}(p_3, m_{\mu}) (-ie\gamma_{\nu}) S_{\mu}(p_1 - p_4 + k) (-ie\gamma_{\mu}) u(p_1, m_{\mu}) S_{\gamma}(p_4 - k) S_{\gamma}(k - p_2) \\ &\quad \times \bar{u}(p_4, m_N) \Gamma_{\gamma NN}^{\mu}(p_4 - k) S_p(k) \Gamma_{\gamma NN}^{\nu}(k - p_2) u(p_2, m_N), \\ i\mathcal{M}_{\mu p}^{(c)} &= \int \frac{d^4 k}{(2\pi)^4} \bar{u}(p_3, m_{\mu}) (-ie\gamma_{\mu}) S_{\mu}(p_1 + p_2 - k) (-ie\gamma_{\nu}) u(p_1, m_{\mu}) S_{\gamma}(p_4 - k) S_{\gamma}(k - p_2) \\ &\quad \times \bar{u}(p_4, m_N) \Gamma_{\gamma \Delta \rightarrow N}^{\mu\alpha}(k, p_4 - k) S_{\Delta, \alpha\beta} \Gamma_{\gamma N \rightarrow \Delta}^{\nu\beta}(k, k - p_2) u(p_2, m_N), \\ i\mathcal{M}_{\mu p}^{(d)} &= \int \frac{d^4 k}{(2\pi)^4} \bar{u}(p_3, m_{\mu}) (-ie\gamma_{\nu}) S_{\mu}(p_1 - p_4 + k) (-ie\gamma_{\mu}) u(p_1, m_{\mu}) S_{\gamma}(p_4 - k) S_{\gamma}(k - p_2) \\ &\quad \times \bar{u}(p_4, m_N) \Gamma_{\gamma \Delta \rightarrow N}^{\mu\alpha}(k, p_4 - k) S_{\Delta, \alpha\beta} \Gamma_{\gamma N \rightarrow \Delta}^{\nu\beta}(k, k - p_2) u(p_2, m_N), \end{aligned} \quad (4)$$

with

$$\begin{aligned} S_{\mu}(\bar{k}) &= \frac{i(\bar{k} + m_{\mu})}{\bar{k}^2 - m_{\mu}^2 + i\epsilon}, \quad S_N(\bar{k}) = \frac{i(\bar{k} + m_N)}{\bar{k}^2 - m_N^2 + i\epsilon}, \\ S_{\Delta, \alpha\beta}(\bar{k}) &= \frac{-i(\bar{k} + m_{\Delta})}{\bar{k}^2 - m_{\Delta}^2 + i\epsilon} P_{\alpha\beta}^{3/2}(\bar{k}), \quad P_{\alpha\beta}^{3/2}(\bar{k}) = g_{\alpha\beta} - \frac{\gamma_{\alpha} \gamma_{\beta}}{3} - \frac{(\bar{k} \gamma_{\alpha} \bar{k}_{\beta} + \bar{k}_{\alpha} \gamma_{\beta} \bar{k})}{3\bar{k}^2}. \end{aligned} \quad (5)$$

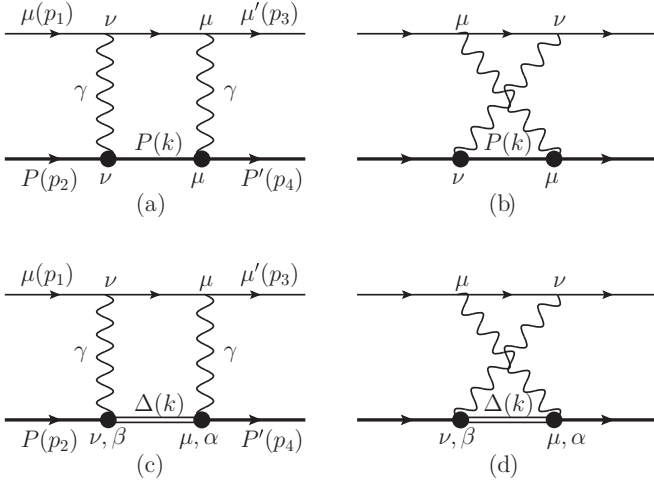


FIG. 2. TPE contributions to  $\mu p$  scattering from the  $s, u$  channels owing to the  $N, \Delta$  intermediate states in Feynman gauge.

### B. TPE contribution from the $\sigma$ intermediate state in the $t$ channel

The meson exchange effect in lepton-proton scattering was first studied in the  $ep$  scattering case in Ref. [32], where it was pointed out that with the current precise experimental data sets at  $Q^2 \equiv -q^2 \sim 2.5 \text{ GeV}^2$  [33–35], the contribution from the  $2^{++}$  meson exchange should be considered. In the  $ep$  scattering case, when  $Q^2 \gg m_e^2$  and the approximation  $m_e = 0$  is taken, the contributions from the  $0^{-+}$  and  $0^{++}$  mesons exchange are zero owing to the zero mass  $m_e$ . In the  $\mu p$  system, these contributions possibly play a role. The contribution from the  $0^{-+}$  meson (pion) in the Lamb shift of the  $\mu p$  system has been discussed in Refs. [11,12] and is found to be very small owing to the chiral anomaly. Recently, the contributions from the  $\sigma$  meson in  $\mu p$  scattering and  $\mu p$  bound states were discussed in Ref. [31] and Ref. [36]. In Ref. [31], the contribution from the  $\sigma$  meson exchange is calculated based on the direct effective coupling of  $\sigma\gamma\gamma$  with a coupling constant  $g_{\sigma\gamma\gamma}$  (for the real photon case). The  $q_\sigma^2$  independent effective coupling constant  $g_{\sigma\gamma\gamma}$  (where  $q_\sigma$  is the four-momentum of the  $\sigma$ ) is determined from the decay width  $\Gamma_{\sigma \rightarrow 2\gamma}$ . This is not a good way for two reasons: (1) The sign of the effective coupling  $g_{\sigma\gamma\gamma}$  cannot be determined just from the decay width  $\Gamma_{\sigma \rightarrow 2\gamma}$ ; (2) the effective coupling  $g_{\sigma\gamma\gamma}$  in the spacelike region is very different from that

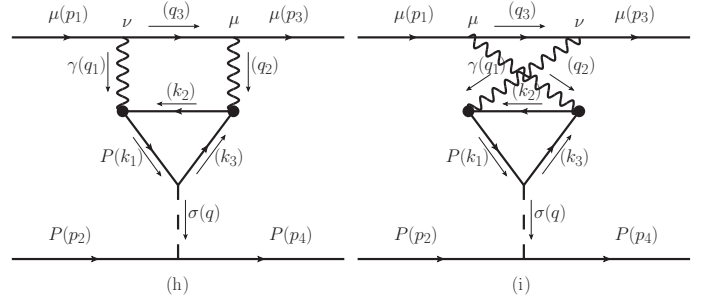


FIG. 4.  $\sigma$  meson exchange between muons and protons with photon and proton loops, (h) boxlike diagram; (i) crossed-box-like diagram.

in the timelike region. For example, it is real in the spacelike region while it is complex in the timelike region when  $q_\sigma^2 > 4m_\pi^2$ . In Ref. [36], the contribution from the  $\sigma$  meson exchange is estimated from the  $\sigma\pi\pi$  and  $\sigma NN$  couplings by the loop effects where the  $q_\sigma^2$  dependence of the effective coupling is included. In this work, I follow the method used in Ref. [36] and take the following effective vertexes to estimate the TPE contribution in the  $\mu p$  scattering owing to the  $\sigma$  meson exchange,

$$\begin{aligned} \tilde{\Gamma}_{\sigma NN} &= -ig_{\sigma NN}, & \tilde{\Gamma}_{\sigma\pi\pi} &= -ig_{\sigma\pi\pi}, \\ \tilde{\Gamma}_{\gamma\pi\pi}^\mu &= -ie(p_1^\mu + p_2^\mu)F_\pi(\bar{q}^2), \\ \tilde{\Gamma}_{\gamma\gamma\pi\pi}^{\mu\nu} &= 2ie^2g^{\mu\nu}F_\pi(q_1^2)F_\pi(q_2^2), \end{aligned} \quad (6)$$

where  $\boldsymbol{\pi} = (\pi_1, \pi_2, \pi_3)$ ,  $\pi^\pm = \frac{\sqrt{2}}{2}(\pi_1 \pm i\pi_2)$ ,  $\pi^0 = \pi_3$ ,  $D_\mu = \partial_\mu + ieA_\mu$ , and  $\bar{q}, q_{1,2}$  are the momenta of the photons. For the effective vertex  $\Gamma_{\gamma NN}^\mu$ , in principle, one should take it as that used in Eq. (3), while in practice, such a choice of the effective vertex leads to too-complex calculation in the two-loop diagrams. Hence, I approximate it as follows when discussing the TPE contribution from the  $\sigma$  meson [36]:

$$\Gamma_{\gamma NN}^\mu \approx \tilde{\Gamma}_{\gamma NN}^\mu = ie\gamma^\mu F_N(\bar{q}^2). \quad (7)$$

With these effective interactions, the corresponding TPE amplitudes can be written from the diagrams shown in Figs. 3 and 4,

$$i\mathcal{M}_{\mu p \rightarrow \mu p}^{(j)} = (i\mathcal{M}_{\mu \rightarrow \mu\sigma^*}^{(j)}) \frac{i}{q^2 - m_\sigma^2 + i\epsilon} (i\mathcal{M}_{p\sigma^* \rightarrow p}), \quad (8)$$

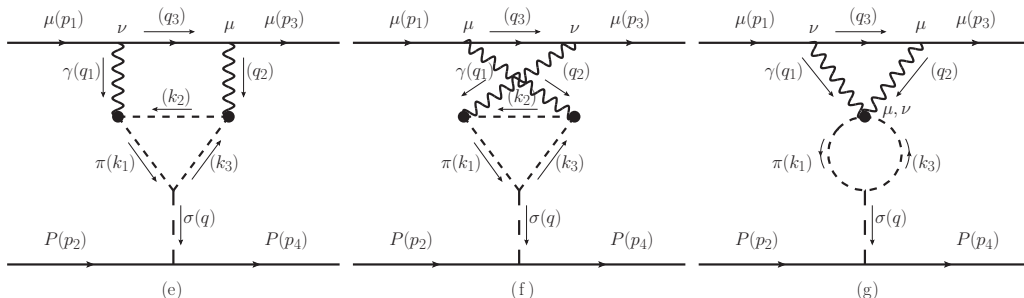


FIG. 3.  $\sigma$  meson exchange between muons and protons with photon and pion loops, (e) boxlike diagram; (f) crossed-box-like diagram; (g) contactlike diagram.

where  $j = (e, f, g, h, i)$ ,  $m_\sigma$  is the mass of the  $\sigma$  meson, and

$$i\mathcal{M}_{p\sigma^* \rightarrow p} = \bar{u}(p_4, m_N) \tilde{\Gamma}_{\sigma NN} u(p_2, m_N). \quad (9)$$

In the Feynman gauge one obtains

$$\begin{aligned} i\mathcal{M}_{\mu \rightarrow \mu\sigma^*}^{(e)} &= \int \frac{d^4 k_1 d^4 k_2}{(2\pi)^8} \bar{u}(p_3, m_\mu) (-ie\gamma_\mu) S_l(q_3) (-ie\gamma_\nu) \\ &\quad \times u(p_1, m_\mu) S_\gamma(q_1) S_\gamma(q_2) \\ &\quad \times S_\pi(k_1) S_\pi(k_2) S_\pi(k_3) \tilde{\Gamma}_{\gamma\pi\pi}^\mu(q_1) \tilde{\Gamma}_{\gamma\pi\pi}^\nu(q_2) \tilde{\Gamma}_{\sigma\pi\pi}, \\ i\mathcal{M}_{\mu \rightarrow \mu\sigma^*}^{(f)} &= \int \frac{d^4 k_1 d^4 k_2}{(2\pi)^8} \bar{u}(p_3, m_\mu) (-ie\gamma_\nu) S_l(q_3) (-ie\gamma_\mu) \\ &\quad \times u(p_1, m_\mu) S_\gamma(q_1) S_\gamma(q_2) \\ &\quad \times S_\pi(k_1) S_\pi(k_2) S_\pi(k_3) \tilde{\Gamma}_{\gamma\pi\pi}^\mu(q_1) \tilde{\Gamma}_{\gamma\pi\pi}^\nu(q_2) \tilde{\Gamma}_{\sigma\pi\pi}, \\ i\mathcal{M}_{\mu \rightarrow \mu\sigma^*}^{(g)} &= \int \frac{d^4 k_1 d^4 k_2}{(2\pi)^8} \bar{u}(p_3, m_\mu) (-ie\gamma_\mu) S_l(q_3) (-ie\gamma_\nu) \\ &\quad \times u(p_1, m_\mu) S_\gamma(q_1) S_\gamma(q_2) \\ &\quad \times S_\pi(k_1) S_\pi(k_2) \tilde{\Gamma}_{\gamma\pi\pi}^{\mu\nu} \tilde{\Gamma}_{\sigma\pi\pi}, \\ i\mathcal{M}_{l \rightarrow l\sigma^*}^{(h)} &= \int \frac{d^4 k_1 d^4 k_2}{(2\pi)^8} \bar{u}(p_3, m_\mu) (-ie\gamma_\mu) S_l(q_3) (-ie\gamma_\nu) \\ &\quad \times u(p_1, m_\mu) S_\gamma(q_1) S_\gamma(q_2) (-1) \text{Tr}[S_N(k_1)] \\ &\quad \times \tilde{\Gamma}_{\gamma NN}^\nu(q_1) S_N(k_2) \tilde{\Gamma}_{\gamma NN}^\mu(q_2) S_N(k_3) \tilde{\Gamma}_{\sigma NN}, \\ i\mathcal{M}_{l \rightarrow l\sigma^*}^{(i)} &= \int \frac{d^4 k_1 d^4 k_2}{(2\pi)^8} \bar{u}(p_3, m_\mu) (-ie\gamma_\nu) S_l(q_3) (-ie\gamma_\mu) \\ &\quad \times u(p_1, m_\mu) S_\gamma(q_1) S_\gamma(q_2) (-1) \text{Tr}[S_N(k_1)] \\ &\quad \times \tilde{\Gamma}_{\gamma NN}^\nu(q_1) S_N(k_2) \tilde{\Gamma}_{\gamma NN}^\mu(q_2) S_N(k_3) \tilde{\Gamma}_{\sigma NN}, \end{aligned} \quad (10)$$

with

$$S_\pi(\bar{k}) = \frac{i}{\bar{k}^2 - m_\pi^2 + i\epsilon}, \quad (11)$$

where  $m_\pi$  is the mass of the pion and  $q_{1,2,3}$  and  $k_{1,2}$  are the corresponding momenta of the photons, pions, and protons shown in the corresponding diagrams of Figs. 3 and 4.

For comparison, I also define the following effective couplings,

$$\begin{aligned} i\mathcal{M}_{\mu \rightarrow \mu\sigma^*}^{(e+f+g)} &\equiv \bar{u}(p_3, m_\mu) (-ig_{\sigma\mu\mu}^{(\pi)}) u(p_1, m_\mu), \\ i\mathcal{M}_{\mu \rightarrow \mu\sigma^*}^{(h+i)} &\equiv \bar{u}(p_3, m_\mu) (-ig_{\sigma\mu\mu}^{(N)}) u(p_1, m_\mu), \end{aligned} \quad (12)$$

and these effective couplings  $g_{\sigma\mu\mu}^{(\pi, N)}$  can be compared directly with the  $f_s$  defined in Ref. [31].

### III. THE INPUT PARAMETERS

#### A. Input parameters for $N, \Delta$ intermediate states in the $s$ and $u$ channels

For the form factors  $F_{1,2}$  in the vertex  $\Gamma_{\gamma NN}^\mu$ , I take a form as in Ref. [16],

$$F_{1,2}(\bar{q}^2) = \sum_{i=1}^3 \frac{n_i}{d_i - \bar{q}^2}, \quad (13)$$

where the parameters  $n_i$  and  $d_i$  for the  $F_1$  and  $F_2$  form factors of the proton can be found in Table I of Ref. [16]. Compared with the calculations in Refs. [17,18], the choice of the form factors is improved.

The  $\Delta$  form factors are taken as those used in Ref. [37],

$$\begin{aligned} F_\Delta^{(1)} &= F_\Delta^{(2)} = \left( \frac{-\Lambda_1^2}{\bar{q}^2 - \Lambda_1^2} \right)^2 \frac{-\Lambda_3^2}{\bar{q}^2 - \Lambda_3^2}, \\ F_\Delta^{(3)} &= \left( \frac{-\Lambda_1^2}{\bar{q}^2 - \Lambda_1^2} \right)^2 \frac{-\Lambda_3^2}{\bar{q}^2 - \Lambda_3^2} \left[ a \frac{-\Lambda_2^2}{\bar{q}^2 - \Lambda_2^2} + (1-a) \frac{-\Lambda_4^2}{\bar{q}^2 - \Lambda_4^2} \right], \end{aligned} \quad (14)$$

with  $\Lambda_1 = 0.84$  GeV,  $\Lambda_2 = 2$  GeV,  $\Lambda_3 = \sqrt{2}$  GeV,  $\Lambda_4 = 0.2$  GeV, and  $a = -0.3$ . The other parameters are taken as  $(g_1, g_2, g_3) = (6.59, 9.08, 7.12)$ . The detail of such choice can be found in Ref. [37].

#### B. Input parameters for $\sigma$ intermediate state in the $t$ channel

For the form factor of the pion, I simply take it as  $F_\pi(\bar{q}^2) = -\Lambda^2/(\bar{q}^2 - \Lambda^2)$ , with  $\Lambda = 0.77$  GeV [38]; for the same reasons I also take  $F_N(\bar{q}^2) = F_\pi(\bar{q}^2)$ .

For  $g_{\sigma NN}$  and  $m_\sigma$ , their values can be found in much of the literature on the nucleon-nucleon potential, and I list some of these [39–42] in the Table I, where one can see there is about 20% difference between the values for  $g_{\sigma NN}$  and  $m_\sigma$ . For simplicity, I take the values in Ref. [39] for the estimation. I also want to point out that the value of  $m_\sigma$  can be different with the pole mass of  $\sigma$ , and it should be understood as the effective or running mass of  $\sigma$  in the  $t$  channel.

For  $g_{\sigma\pi\pi}$ , I take its form as  $g_{\sigma\pi\pi}(Q^2) = \tilde{g}_{\sigma\pi\pi} \frac{\Lambda_\sigma^2 - m_\sigma^2}{\Lambda_\sigma^2 + Q^2}$  and match  $g_{\sigma\pi\pi}(0)$  with B $\chi$ PT [10] by  $g_{\sigma\pi\pi}(0)g_{\sigma NN}(0)/m_\sigma^2 = g_A^2 m_N / f_\pi^2 \approx 177$  GeV $^{-1}$ , which gives  $\tilde{g}_{\sigma\pi\pi} = 6.14$  GeV.

TABLE I. Values of  $m_\sigma$ ,  $g_{\sigma NN}$ , and  $\Lambda_\sigma$  used in Ref. [39] (Table 5) and Refs. [40–42].

Reference	$m_\sigma$ (GeV)	$g_{\sigma NN}(Q^2)$	$\Lambda_\sigma$ (GeV)	$g_{\sigma NN}^2(Q^2=0)/m_\sigma^2$ (GeV $^{-2}$ )
[39] (Table 5)	0.550	$10.20 \frac{\Lambda_\sigma^2 - m_\sigma^2}{\Lambda_\sigma^2 + Q^2}$	2.0	294
[40]	0.650	$12.78 \frac{\Lambda_\sigma^2 - m_\sigma^2}{\Lambda_\sigma^2 + Q^2}$	1.7	282
[41]	0.5325	$10.581 \frac{\Lambda_\sigma^2 - m_\sigma^2}{\Lambda_\sigma^2 + Q^2}$	2	356
[42]	0.65	$13.85 \frac{\Lambda_\sigma^2 - m_\sigma^2}{\Lambda_\sigma^2 + Q^2}$	1.8	343

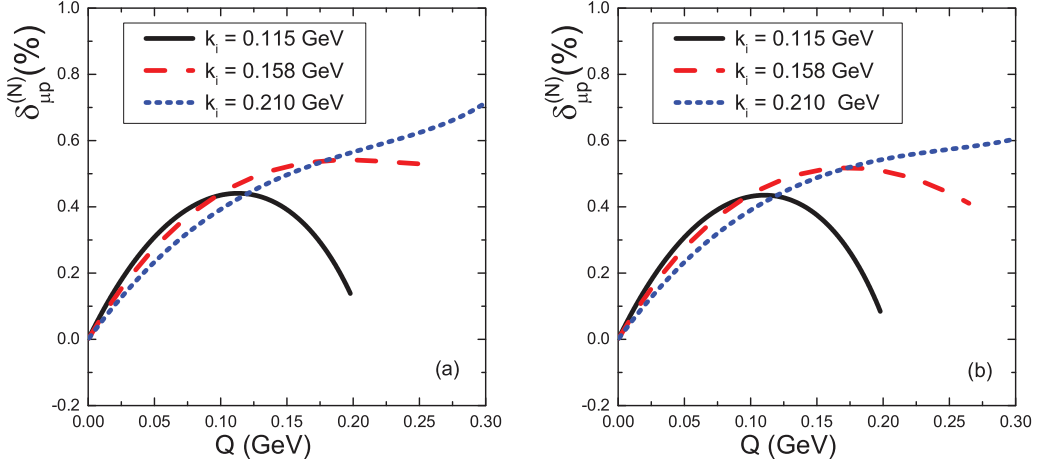


FIG. 5. TPE corrections from the  $N$  intermediate state  $\delta_{\mu p}^{(N)}$  as a function of  $Q$  at  $k_i = 0.115, 0.158, 0.21$  GeV, with  $k_i$  the three-momentum of the initial muon in the laboratory frame. (a) The corrections using Eq. (13) as input; (b) the corrections using Eq. (18) of Ref. [10] as input.

#### IV. NUMERICAL RESULTS

We use the package FEYNALC [43] to deal with the analytical part of the calculation, use LOOPTOOLS [44] to do the numerical integration for one-loop diagrams, and use FIESTA4 [45] to do the numerical integration for the two-loop diagrams.

##### A. Numerical results for TPE corrections from the $N$ intermediate state

Using the expression of the amplitudes, one can get the corresponding cross sections directly as

$$\begin{aligned} \sigma_{\mu p}^{1\gamma} &= C_{\mu p} \sum |\mathcal{M}_{\mu p}^{(1\gamma)}|^2, \\ \sigma_{\mu p}^{1\gamma+2\gamma(N)} &\equiv C_{\mu p} \sum \{ |\mathcal{M}_{\mu p}^{(1\gamma)}|^2 \\ &\quad + 2\text{Re}[\mathcal{M}_{\mu p}^{(1\gamma)*}(\mathcal{M}_{\mu p}^{(a+b)} - \mathcal{M}_{\text{IR},\mu p}^{(\text{MT})})] \} \\ &\equiv \sigma_{\mu p}^{1\gamma} [1 + \delta_{\mu p}^{(N,\text{full})} - \delta_{\text{IR},\mu p}^{(\text{MT})}] \\ &\equiv \sigma_{\mu p}^{1\gamma} [1 + \delta_{\mu p}^{(N)}], \end{aligned} \quad (15)$$

where  $C_{\mu p}$  is a global factor related to the phase space,  $\mathcal{M}_{\text{IR},\mu p}^{(\text{MT})}$  refers to the IR part of the amplitudes separated by the Mo and Tsai method [46],  $\delta_{\text{IR},\mu p}^{(\text{MT})}$  is the corresponding correction to the cross section, and its explicit expressions can be found in Ref. [14].

The numerical results for  $\delta_{\mu p}^{(N)}$  vs  $Q$  at fixed  $k_i$  are presented in Fig. 5(a), where  $k_i$  is the magnitude of the three-momentum of the initial muon in the laboratory frame. Here I use  $Q$  but not  $Q^2$  as the  $x$  coordinate owing to the advantage in the following

TABLE II. Numerical results for the parameters  $c_i^{(N)}$ ; the units for both  $k_i$  and  $Q$  are GeV in the fitting to obtain  $c_i^{(N)}$ .

$c_{1,\mu p}^{(N)}$	15.2205	$c_{4,\mu p}^{(N)}$	52.5231	$c_{7,\mu p}^{(N)}$	91.8465
$c_{2,\mu p}^{(N)}$	-70.787	$c_{5,\mu p}^{(N)}$	-113.801	$c_{8,\mu p}^{(N)}$	-416.08
$c_{3,\mu p}^{(N)}$	118.222	$c_{6,\mu p}^{(N)}$	-10.1527	$c_{9,\mu p}^{(N)}$	592.395

fitting. Also, one should note that when  $k_i$  is fixed, there is a maximum value for  $Q$ .

In addition, I fit the TPE corrections  $\delta_{\mu p}^{(N)}$  at small  $k_i$  and  $Q$  using the following naive formula:

$$\begin{aligned} \delta_{\mu p}^{(N)}(Q^2, k_i) &= [c_{1,\mu p}^{(N)} + c_{2,\mu p}^{(N)}k_i + c_{3,\mu p}^{(N)}k_i^2]Q \\ &\quad + [c_{4,\mu p}^{(N)} + c_{5,\mu p}^{(N)}k_i + c_{6,\mu p}^{(N)}/k_i]Q^2 \\ &\quad + [c_{7,\mu p}^{(N)} + c_{8,\mu p}^{(N)}k_i + c_{9,\mu p}^{(N)}k_i^2]Q^3. \end{aligned} \quad (16)$$

The numerical results for the fitted parameters are listed in Table II. With these parameters, the  $\delta_{\mu p}^{(N)}$  in the full region with  $k_i \subseteq [0.01, 0.3]$  GeV and  $Q \leq 0.4$  GeV can be well reproduced and this formula can be used directly to estimate

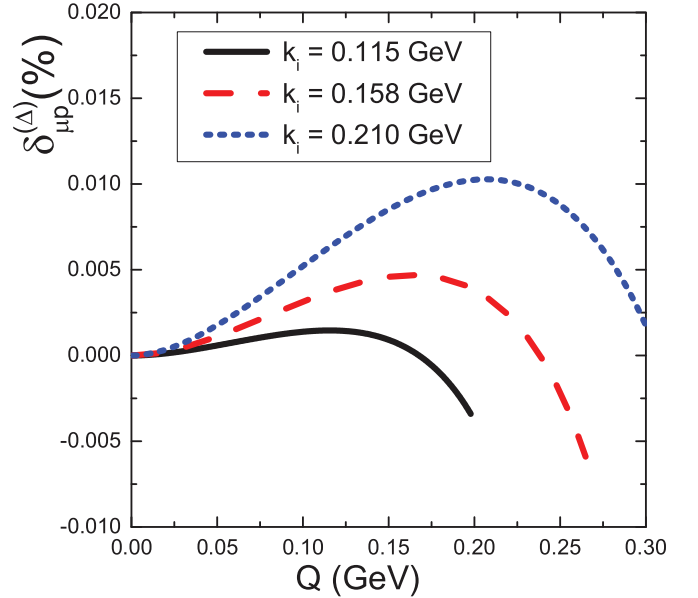


FIG. 6. TPE corrections from the  $\Delta$  intermediate state  $\delta_{\mu p}^{(\Delta)}$  vs  $Q$  at  $k_i = 0.115, 0.158, 0.21$  GeV with  $k_i$  the three-momentum of the initial muon in the laboratory frame.

TABLE III. Numerical results for the parameters  $c_i^{(\Delta)}$ ; the units for both  $k_i$  and  $Q$  are GeV in the fitting to obtain  $c_i^{(\Delta)}$ .

$c_{1,\mu p}^{(\Delta)}$	-0.1314	$c_{4,\mu p}^{(\Delta)}$	0.3633	$c_{7,\mu p}^{(\Delta)}$	-19.2295
$c_{2,\mu p}^{(\Delta)}$	1.0377	$c_{5,\mu p}^{(\Delta)}$	28.2938	$c_{8,\mu p}^{(\Delta)}$	36.1717
$c_{3,\mu p}^{(\Delta)}$	-0.7978	$c_{6,\mu p}^{(\Delta)}$	-71.6715	$c_{9,\mu p}^{(\Delta)}$	18.0616

the TPE correction from the  $N$  intermediate state in the above momentum region within the model.

For comparison, in Fig. 5(b) I also present the numerical results using the form factors of Eq. (18) of Ref. [18] as input. The numerical results obtained here are the same as those given in Ref. [18] when  $\epsilon < 1$ , while I find there is a sign difference when  $\epsilon > 1$ , where the definition of  $\epsilon$  can be found in Ref. [18].

### B. Numerical results for TPE corrections from the $\Delta$ intermediate state

Similar to the  $N$  case, I define

$$\begin{aligned} \sigma_{\mu p}^{1\gamma+2\gamma(\Delta)} &\equiv C_{\mu p} \sum \{ |\mathcal{M}_{\mu p}^{1\gamma}|^2 + 2\text{Re}[\mathcal{M}_{\mu p}^{1\gamma*} \mathcal{M}_{\mu p}^{(c+d)}] \} \\ &\equiv \sigma_{\mu p}^{1\gamma} [1 + \delta_{\mu p}^{(\Delta)}]. \end{aligned} \quad (17)$$

The numerical results for the  $\delta_{\mu p}^{(\Delta)}$  are presented in Fig. 6.

Similarly, I fit  $\delta_{\mu p}^{(\Delta)}$  at small  $k_i$  and  $Q^2$  as

$$\begin{aligned} \delta_{\mu p}^{(\Delta)}(Q^2, k_e) &= [c_{1,\mu p}^{(\Delta)} k_i + c_{2,\mu p}^{(\Delta)} k_i^2 + c_{3,\mu p}^{(\Delta)} k_i^3] Q \\ &\quad + [c_{4,\mu p}^{(\Delta)} k_i + c_{5,\mu p}^{(\Delta)} k_i^2 + c_{6,\mu p}^{(\Delta)} k_i^3] Q^2 \\ &\quad + [c_{7,\mu p}^{(\Delta)} k_i + c_{8,\mu p}^{(\Delta)} k_i^2 + c_{9,\mu p}^{(\Delta)} k_i^3] Q^3. \end{aligned} \quad (18)$$

The numerical results for the fitted parameters are listed in Table III. The results in the region with  $k_i \subseteq [0.1, 0.3]$  GeV and  $Q \leq 0.4$  GeV can be well reproduced by this formula and these parameters. The corrections in the region  $k_i < 0.1$  GeV are almost zero, and I do not give a meticulous fitting.

### C. Numerical results for TPE corrections from the $\sigma$ intermediate state in the $t$ channel

To discuss the TPE corrections from the  $\sigma$  meson exchange, I define

$$\begin{aligned} \sigma_{\mu p}^{1\gamma+2\gamma(\sigma,\pi)} &\equiv C_{\mu p} \sum \{ |\mathcal{M}_{\mu p}^{1\gamma}|^2 + 2\text{Re}[\mathcal{M}_{\mu p}^{1\gamma*} \mathcal{M}_{\mu p}^{(e+f+g)}] \} \\ &\equiv \sigma_{\mu p}^{1\gamma} [1 + \delta_{\mu p}^{(\sigma,\pi)}], \\ \sigma_{\mu p}^{1\gamma+2\gamma(\sigma,N)} &\equiv C_{\mu p} \sum \{ |\mathcal{M}_{\mu p}^{1\gamma}|^2 + 2\text{Re}[\mathcal{M}_{\mu p}^{1\gamma*} \mathcal{M}_{\mu p}^{(h+i)}] \} \\ &\equiv \sigma_{\mu p}^{1\gamma} [1 + \delta_{\mu p}^{(\sigma,N)}]. \end{aligned} \quad (19)$$

The numerical results for  $\delta_{\mu p}^{(\sigma,(\pi+N))}$  vs  $Q$  are presented in the left panel of Fig. 7, and the results  $\delta_{\mu p}^{(\sigma,(\pi+N))}$  vs  $\theta_{\text{lab}}$ , which can be compared directly with Fig. 5 of Ref. [31], are presented in the right panel of Fig. 7, where  $\theta_{\text{lab}}$  is the scattering angle of the muon in the laboratory frame. One should note that there is a sign difference between the definition of  $\delta_{\mu p}^{(\sigma,(\pi+N))}$  in Eq. (19) and that in Eq. (22) of Ref. [31].

Unlike the  $N, \Delta$  cases, the dependence of the TPE corrections from the  $\sigma$  meson exchange on the effective coupling  $g_{\sigma\mu\mu}^{(\pi,N)}$  can be expressed in an explicit form [31]. So I do not fit the dependence of  $\delta_{\mu p}^{(\pi+N)}$  on  $k_i$  and  $Q$ , but express the  $g_{\sigma\mu\mu}^{(\pi,N)}$  at small  $Q$  as

$$\begin{aligned} g_{\sigma\mu\mu}^{(\pi)}(Q^2) &= [c_0^{(\pi)} + c_1^{(\pi)} Q + c_2^{(\pi)} Q^2 + c_3^{(\pi)} Q^3] g_{\sigma\pi\pi}, \\ g_{\sigma\mu\mu}^{(N)}(Q^2) &= [c_0^{(N)} + c_1^{(N)} Q + c_2^{(N)} Q^2 + c_3^{(N)} Q^3] g_{\sigma NN}, \end{aligned} \quad (20)$$

and I take  $c_{1,2}^{(\pi,N)}$  from Ref. [36], where the function SDEX-PANDASY in FIESTA is used to calculate and fit  $c_{3,4}^{(\pi,N)}$  from the  $g_{\sigma\mu\mu}^{(\pi,N)}$  in the region  $Q \subseteq [0.01, 0.4]$  GeV, and at last one has the parameters as in Table IV. With these parameters, the behavior of  $g_{\sigma\mu\mu}^{(\pi,N)}$  at  $Q \leq 0.4$  GeV can be well reproduced. We should note that the  $c_{0,1,2,3}^{(\pi,N)}$  depend only on the masses of muon, pion, and proton and on the corresponding form factors in  $\Gamma_{\gamma\pi\pi}^\mu$  and  $\Gamma_{\gamma NN}^\mu$ . The  $\sigma$ -related property is included in the factors  $g_{\sigma\pi\pi}$  and  $g_{\sigma NN}$ .

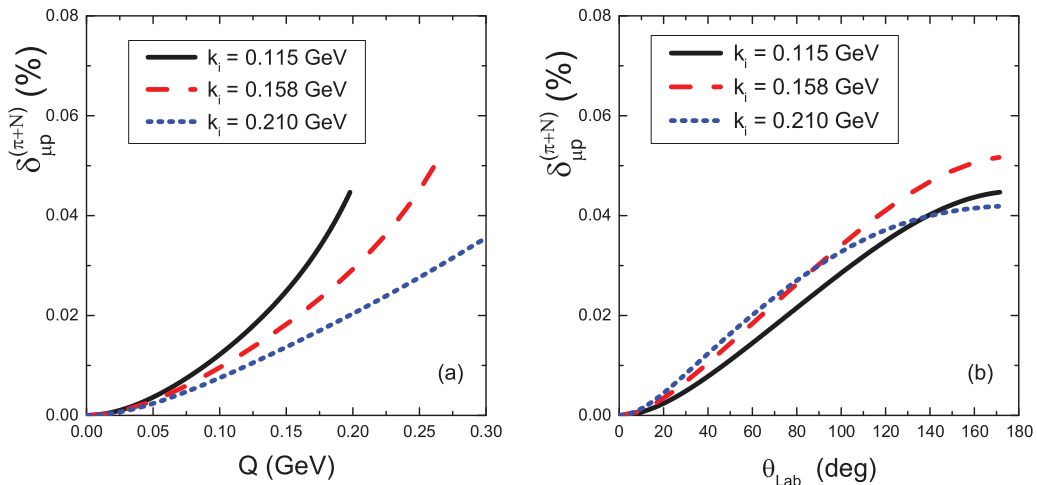


FIG. 7. TPE corrections from the  $\sigma$  intermediate state  $\delta_{\mu p}^{(\sigma,(\pi+N))}$  at  $k_i = 0.115, 0.158, 0.21$  GeV with  $k_i$  the three-momentum of the initial muon in the laboratory frame. (a)  $\delta_{\mu p}^{(\sigma,(\pi+N))}$  vs  $Q$ ; (b)  $\delta_{\mu p}^{(\sigma,(\pi+N))}$  vs  $\theta_{\text{lab}}$ .

TABLE IV. Numerical results for the parameters  $c_j^{(i)}$  with  $j = 0, 1, 2, 3$  and  $i = \pi, N$ ; the unit for  $Q$  is GeV in the fitting to obtain  $c_j^{(i)}$ .

	$c_0^{(i)}$	$c_1^{(i)}$	$c_2^{(i)}$	$c_3^{(i)}$
$i = \pi$	5.2770	-28.7494	67.1914	-64.4362
$i = N$	1.0755	-4.7336	12.3169	-14.7901

To compare with the effective coupling  $f_s$  defined in Ref. [31], I also present the  $Q^2$  dependence of  $g_{\sigma\mu\mu}^{(\pi, N, \pi+N)}$  in Fig. 8.

#### D. Discussion and summary

The numerical results presented in Fig. 5 show that the TPE corrections from the  $N$  intermediate state are almost independent of the input form factors when  $Q < 0.2$  GeV and  $k_i < 0.21$  GeV; this is natural because the different input form factors are almost the same at very low-momentum transfer. When  $k_i = 0.21$  GeV and  $Q = 0.3$  GeV, there is a sizable difference (about 15% difference) between these results and those in Ref. [18], which means that a careful choice of the form factors is meaningful when  $Q > 0.25$  GeV. The naive formula Eq. (16) can be used directly for other analysis in the region, with  $k_i \subseteq [0.01, 0.3]$  GeV and  $Q \leq 0.4$  GeV.

The corrections from the  $\Delta$  intermediate state at low-momentum transfer are much smaller than that from the  $N$  intermediate state, and can be neglected when  $k_i < 0.158$  GeV, and even when  $k_i = 0.21$  GeV and  $Q \sim 0.22$  GeV the correction is about 2% of that from the  $N$  intermediate state. Comparing these results with the corrections from the inelastic state estimated by Ref. [47], one can see that the magnitudes are of the same order, while the results in this work are smaller

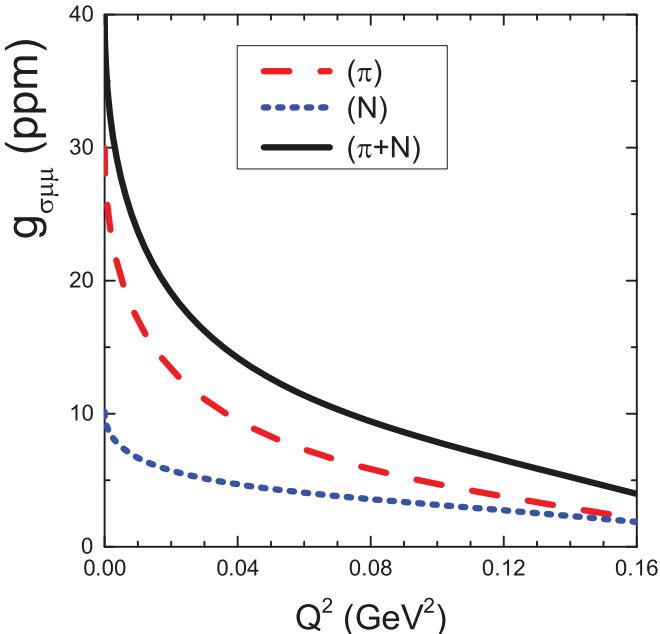


FIG. 8. Numerical results for  $g_{\sigma\mu\mu}$  vs  $Q^2$ , which can be compared directly with the  $f_s$  in Ref. [31]; ppm means  $10^{-6}$ .

than theirs. The reason for this difference may be attributed to the effects from the  $\pi N$  inelastic state and the decay width of  $\Delta$ . Because in the discussed momentum transfer region this correction is much smaller than that from the  $N$  intermediate state, I do not discuss this in detail.

For the corrections from the  $\sigma$  meson exchange  $\delta_{\mu p}^{(\sigma, \pi+N)}$ , the general property of the results in this work and those in Ref. [31] is similar when  $k_i = 0.115, 0.158, 0.21$  GeV. For the effective coupling  $g_{\sigma\mu\mu}$  one can find that at small  $Q^2$  the results in this work are similar to the results shown in Fig. 4 of Ref. [31], while at  $Q^2 = 0.16$  GeV<sup>2</sup>, one finds that the results in this work are only about half of that given in Ref. [31] (shaded region). In other words,  $g_{\sigma\mu\mu}$  decreases much faster than that estimated in Ref. [31].

In summary, in this work, the TPE corrections to unpolarized  $\mu p$  scattering owing to the  $N, \Delta$  and the  $\sigma$  intermediate states are discussed in the hadronic model. One finds at small  $k_i$  and  $Q^2$  that the corrections from the  $N$  intermediate state are dominant, and the corrections from the  $\Delta$  and the  $\sigma$  intermediate states are smaller than 0.05%. This property is the same as in the calculation given in the literature using other methods. In this work, the form factors for  $\gamma NN$  are improved to estimate the corrections from the  $N$  intermediate state and a naive formula which can well reproduce the corrections in the region with  $k_i \subseteq [0.01, 0.3]$  GeV and  $Q \leq 0.4$  GeV is given.

#### ACKNOWLEDGMENTS

This work is supported by the National Natural Science Foundations of China under Grant No. 11375044 and in part by the Fundamental Research Funds for the Central Universities under Grant No. 2242014R30012. The author thanks A.V. Smirnov and Wen-Long Sang for the help on FIESTA and Shin Nan Yang for the helpful suggestion.

#### APPENDIX: SOME RELATIONS

In this Appendix, I list the relations between some quantities used in the literature, and I take  $k_i$  and  $Q$  as the basic variables,

$$\begin{aligned}
 Q_{\max}^2 &= \frac{4m_N^2 k_i^2}{2E_i m_N + m_N^2 + m_\mu^2}, \\
 \cos\theta_{\text{lab}} &= \frac{2m_N k_i^2 - Q^2(E_i + m_N)}{k_i \sqrt{4m_N^2 k_i^2 - 4E_i m_N Q^2 + Q^4}}, \\
 \tan\frac{\theta_B}{2} &= \frac{Q\sqrt{Q^2 + 4m_N^2}}{2\sqrt{4m_N^2 k_i^2 - Q^2(2E_i m_N + m_N^2 + m_\mu^2)}}, \\
 E_f &= \frac{E_i m_N - Q^2}{2m_N}, \\
 \epsilon &\equiv \frac{16v^2 - Q^2(Q^2 + 4m_N^2)}{16v^2 - Q^2(Q^2 + 4m_N^2) + 2(Q^2 + 4m_N^2)(Q^2 - 2m_\mu^2)},
 \end{aligned} \tag{A1}$$

where  $E_i = \sqrt{k_i^2 + m_\mu^2}$ ,  $v = m_N(E_i + E_f)/2$ ,  $\theta_{\text{lab}}$  is the scattering angle of the final muon in the laboratory frame,  $\theta_B$  is the scattering angle in the Breit frame, and the definition of  $\epsilon$  is taken from Ref. [10]. We also have

$$\begin{aligned} \frac{1}{4} \sum_{\text{spin}} |M_{\mu p}^{1\gamma}|^2 &= e^4 (g_1 F_1^2 + g_2 F_2^2 + g_3 F_1 F_2), \\ \frac{1}{4} \sum_{\text{spin}} 2\text{Re}[M_{\mu p}^{1\gamma*} M_{\mu p}^\sigma] &= e^2 g_{\sigma\mu\mu}^{(\pi+N)} g_{\sigma NN} g_4 (4F_1 m_N^2 - F_2 Q^2), \end{aligned} \quad (\text{A2})$$

with

$$\begin{aligned} g_1 &= 2 \left( 1 - \frac{4E_i m_N + 2m_N^2 + 2m_\mu^2}{Q^2} + \frac{8E_i^2 m_N^2}{Q^4} \right), \\ g_2 &= 1 - \frac{2E_i}{m_N} + \frac{4k_i^2}{Q^2}, \\ g_3 &= 4 - \frac{8m_\mu}{Q^2}, \\ g_4 &= \frac{2m_\mu(4E_i m_N - Q^2)}{m_N Q^2 (m_\sigma^2 + Q^2)}. \end{aligned} \quad (\text{A3})$$

- 
- [1] C. E. Carlson and M. Vanderhaeghen, *Ann. Rev. Nucl. Part. Sci.* **57**, 171 (2007).
- [2] J. Arrington, P. Blunden P., and W. Melnitchouk, *Prog. Nucl. Part. Phys.* **66**, 782 (2011).
- [3] L. Andivahis, P. E. Bosted, A. Lung, L. M. Stuart, J. Alster, R. G. Arnold, C. C. Chang, F. S. Dietrich, W. Dodge, R. Gearhart *et al.*, *Phys. Rev. D* **50**, 5491 (1994).
- [4] R. C. Walker, B. W. Filippone, J. Jourdan, R. Milner, R. McKeown, D. Potterveld, L. Andivahis, R. Arnold, D. Benton, P. Bosted *et al.*, *Phys. Rev. D* **49**, 5671 (1994).
- [5] M. K. Jones *et al.* (JLab Hall A Collaboration), *Phys. Rev. Lett.* **84**, 1398 (2000).
- [6] O. Gayou *et al.* (JLab Hall A Collaboration), *Phys. Rev. Lett.* **88**, 092301 (2002).
- [7] R. Pohl *et al.*, *Nature (London)* **466**, 213 (2010).
- [8] A. Antognini *et al.*, *Science* **339**, 417 (2013).
- [9] M. C. Birsea and J. A. McGovern, *Eur. Phys. J. A* **48**, 120 (2012); C. Peset and A. Pineda, *Nucl. Phys. B* **887**, 69 (2014).
- [10] J. M. Alarcon, V. Lensky, and V. Pascalutsa, *Eur. Phys. J. C* **74**, 2852 (2014).
- [11] Hai-Qing Zhou and Hou-Rong Pang, *Phys. Rev. A* **92**, 032512 (2015); **93**, 069903(E) (2016).
- [12] F. Hagelstein and V. Pascalutsa, *PoS CD15*, 077 (2016); N. T. Huang, E. Kou, and B. Moussallam, *Phys. Rev. D* **93**, 114005 (2016).
- [13] K. E. Mesick (MUSE Collaboration), *PoS NUFAC2014*, 091 (2015).
- [14] P. G. Blunden, W. Melnitchouk, and J. A. Tjon, *Phys. Rev. Lett.* **91**, 142304 (2003).
- [15] S. Kondratyuk, P. G. Blunden, W. Melnitchuk, and J. A. Tjon, *Phys. Rev. Lett.* **95**, 172503 (2005).
- [16] P. G. Blunden, W. Melnitchouk, and J. A. Tjon, *Phys. Rev. C* **72**, 034612 (2005).
- [17] Dian-Yong Chen and Yu-Bing Dong, *Phys. Rev. C* **87**, 045209 (2013).
- [18] O. Tomalak and M. Vanderhaeghen, *Phys. Rev. D* **90**, 013006 (2014).
- [19] Y. C. Chen, A. Afanasev, S. J. Brodsky, C. E. Carlson, and M. Vanderhaeghen, *Phys. Rev. Lett.* **93**, 122301 (2004).
- [20] A. V. Afanasev, S. J. Brodsky, C. E. Carlson, Y.-C. Chen, and M. Vanderhaeghen, *Phys. Rev. D* **72**, 013008 (2005).
- [21] Y. C. Chen, C. W. Kao, and S. N. Yang, *Phys. Lett. B* **652**, 269 (2007).
- [22] D. Borisyuk and A. Kobushkin, *Phys. Rev. C* **76**, 022201 (2007).
- [23] D. Borisyuk and A. Kobushkin, *Phys. Rev. C* **78**, 025208 (2008).
- [24] D. Borisyuk and A. Kobushkin, *Phys. Rev. C* **74**, 065203 (2006).
- [25] D. Borisyuk and A. Kobushkin, *Phys. Rev. C* **83**, 025203 (2011).
- [26] D. Borisyuk and A. Kobushkin, *Phys. Rev. C* **86**, 055204 (2012).
- [27] D. Borisyuk and A. Kobushkin, *Phys. Rev. C* **89**, 025204 (2014).
- [28] D. Borisyuk, and A. Kobushkin, *Phys. Rev. D* **79**, 034001 (2009).
- [29] N. Kivel and M. Vanderhaeghen, *Phys. Rev. Lett.* **103**, 092004 (2009).
- [30] N. Kivel and M. Vanderhaeghen, *J. High Energy Phys.* **04** (2013) 029.
- [31] O. Koshchii and A. Afanasev, *Phys. Rev. D* **94**, 116007 (2016).
- [32] Hong-Yu Chen and Hai-Qing Zhou, *Phys. Rev. C* **90**, 045205 (2014).
- [33] I. A. Qattan *et al.*, *Phys. Rev. Lett.* **94**, 142301 (2005).
- [34] I. A. Qattan, [arXiv:nucl-ex/0610006](https://arxiv.org/abs/nucl-ex/0610006).
- [35] M. Meziane *et al.* (Gep  $2\gamma$  Collaboration), *Phys. Rev. Lett.* **106**, 132501 (2011).
- [36] Hai-Qing Zhou, *Phys. Rev. A* **94**, 052335 (2016).
- [37] Hai-Qing Zhou and Shin Nan Yang, *Eur. Phys. J. A* **51**, 105 (2015).
- [38] H. J. Behrend *et al.* (CELLO Collaboration), *Z. Phys. C* **49**, 401 (1991); J. Gronberg *et al.* (CLEO Collaboration), *Phys. Rev. D* **57**, 33 (1998); G. Huber *et al.*, *Phys. Rev. C* **78**, 045203 (2008).
- [39] R. Machleidt, K. Holinde, and C. Elster, *Phys. Rept.* **149**, 1 (1987).
- [40] A. M. Gasparyan, J. Haidenbauer, C. Hanhart, and J. Speth, *Phys. Rev. C* **68**, 045207 (2003).
- [41] A. Calle Cordon and E. Ruiz Arriola, *Phys. Rev. C* **81**, 044002 (2010).
- [42] D. Ronchen, M. Doring, F. Huang, H. Haberzettl, J. Haidenbauer, C. Hanhart, S. Krewald, U.-G. Meisner, and K. Nakayama, *Eur. Phys. J. A* **49**, 44 (2013).
- [43] Vladyslav Shtabovenko, Rolf Mertig, and Frederik Orellana, *Comput. Phys. Commun.* **207**, 432 (2016).
- [44] T. Hahn and M. Perez-Victoria, *Comput. Phys. Commun.* **118**, 153 (1999).
- [45] Alexander V. Smirnov, *Comput. Phys. Commun.* **204**, 189 (2016).
- [46] L. W. Mo and Y. S. Tsai, *Rev. Mod. Phys.* **41**, 205 (1969); Y. S. Tsai, *Phys. Rev.* **122**, 1898 (1961).
- [47] O. Tomalak and M. Vanderhaeghen, *Eur. Phys. J. C* **76**, 125 (2016).